Acta Biomaterialia xxx (2009) xxx–xxx

Contents lists available at ScienceDirect

Acta Biomaterialia

journal homepage: www.elsevier.com/locate/actabiomat

Heparin-immobilized polymers as non-inflammatory and non-thrombogenic coating materials for arsenic trioxide eluting stents

Feirong Gong [a], Xiaoyan Cheng [a], Shanfeng Wang [b,*], Yanchao Zhao [a], Yun Gao [a], Haibo Cai [c]

[a] Key Laboratory for Ultrafine Materials of Ministry of Education, School of Materials Science and Engineering, East China University of Science and Technology, Shanghai 200237, China
[b] Department of Materials Science and Engineering, The University of Tennessee, Knoxville, TN 37996, USA
[c] State Key Laboratory of Bioreactor Engineering, East China University of Science and Technology, Shanghai 200237, China

ARTICLE INFO

Article history:
Received 4 March 2009
Received in revised form 24 June 2009
Accepted 9 July 2009
Available online xxxx

Keywords:
Stent
Biodegradability
Heparin
Arsenic trioxide (As_2O_3)
Restenosis

ABSTRACT

We have synthesized heparin-immobilized copolymers of L-lactide (LA) and 5-methyl-5-benzyloxycarbonate-1,3-dioxan-2-one (MBC) as non-inflammatory and non-thrombogenic biodegradable coating materials. These copolymers were used in fabricating arsenic trioxide (As_2O_3)-eluting stents to reduce the late-stage adverse events, such as thrombosis, localized hypersensitivity and inflammation, that occur when applying stents to treat coronary artery diseases. Heparinized copolymers effectively reduced platelet adhesion and protein adsorption while increasing the plasma recalcification time and thromboplastin time in vitro. Histological analysis of the polymer-coated stents in a porcine coronary artery injury model indicated that one heparinized copolymer (Hep-Co90, LA:MBC = 90:10), with the highest LA content of 90% and the lowest degradation rate, induced the least foreign body reactions and inflammation, which were as small as those induced by bare metal stents. Consequently, Hep-Co90 was used as the stent coating material for local As_2O_3 delivery. Histomorphometric evaluations suggested no significant difference between bare metal stents and As_2O_3-eluting stents at 1 and 3 months post-implantation. At 6 months, the lumen area in the porcine coronary arteries treated with As_2O_3-eluting stents is 32.4% higher than those treated with bare metal stents while the neointimal area, neointimal thickness and stenosis rate decreased by 25.8%, 32.5% and 31.2%, respectively. The As_2O_3-eluting stent using Hep-Co90 as the drug carrier and stent coating material presented in this study represents a novel promising device in preventing in-stent restenosis.

1. Introduction

Implantation of stents is the most effective means to treat symptomatic coronary artery diseases [1]. Drug-eluting stents (DESs) have been attracting tremendous attention as positive trial results indicate their efficacy for preventing restenosis [2]. In the past few years, in-stent restenosis rates following DES placement have been reported to be typically less than 10% [3,4]. However, there remain many limitations about the long-term safety and efficacy of DESs. These safety problems may be generated by polymer coatings and anti-proliferative agents in DESs themselves. Meanwhile, delayed or incomplete endothelialization on the stent surface is believed to be responsible for the significantly higher thrombosis rates in sirolimus (rampamycin)-eluting (Cypher™, Cordis) and paclitaxel-eluting stents (TAXUS™, Boston Scientific) compared with bare metal stents (BMSs) [5–14]. Although slow-releasing DESs may lead to more favorable angiographic outcomes than rapid-releasing stents [6], sustained release of the drug over a longer period, such as >1 month, delays healing. Furthermore, the long-term existence of a biostable but not truly biocompatible polymer coating stimulates additional foreign body reactions and consequently increases the possibilities of vital late-stage restenosis and thrombosis. Based on the correlation between surface properties and long-term implantation results, it has been suggested that a drug-loaded biocompatible and biodegradable polymer coating on BMSs may reduce late-stage adverse events such as thrombosis, localized hypersensitivity and inflammation [15].

Therefore, the biocompatibility of polymer coatings, as manifested by low thrombogenicity and little induction of foreign body reaction, are crucial in determining the performance of DESs [16]. Heparin is an anticoagulant agent that can interact with antithrombin III to prevent thrombus formation and activation [17]. Heparin-coated stents were reported to be desirable in reducing stent thrombosis and proliferative vascular response; however, they did not show superiority on restenosis over standard BMSs [18,19]. Arsenic trioxide (As_2O_3) has been used to treat acute promyelocytic leukemia and As_2O_3-eluting stents with a rapid-release

* Corresponding author. Tel.: +1 865 974 7809; fax: +1 865 974 4115.
E-mail address: swang16@utk.edu (S. Wang).

1742-7061/$ - see front matter © 2009 Acta Materialia Inc. Published by Elsevier Ltd. All rights reserved.
doi:10.1016/j.actbio.2009.07.013

profile have been fabricated to effectively reduce neointimal thickening in a rabbit iliac artery injury model [20]. Stents coated with 40 μg of As_2O_3 per stent were similar to those coated with 180 μg of paclitaxel in inhibiting neointimal proliferation in the rabbit model and only a mildly delayed endothelialization was found [20]. No more severe inflammation was found up to 28 days after stenting [20].

In this report, we present three heparin-immobilized (or heparinized) copolymers of L-lactide (LA) and 5-methyl-5-benzyloxycarbonate-1,3-dioxan-2-one (MBC) with different LA contents, poly(LA-*co*-MBC) (PLM), as non-inflammatory and non-thrombogenic biodegradable coating materials for fabricating As_2O_3-eluting stents. The surface heparin contents, physical properties, surface morphology, in vitro hydrolytical degradation and heparin release profiles of these heparinized-copolymer-coated stents have been investigated and correlated with their in vivo performance. Stents coated with these heparinized copolymers and As_2O_3-eluting stents have been implanted, evaluated using a porcine coronary artery injury model and compared with BMSs and stents coated with one PLM copolymer.

2. Materials and methods

2.1. Synthesis of heparin-immobilized polymers

MBC monomer was synthesized using the method described in Ref. [21]. As depicted in Fig. 1, PLM was prepared via the ring-opening polymerization of LA and MBC at 110 °C for 24 h in the presence of stannous (II) 2-ethylhexanoate ($Sn(Oct)_2$). Purification was carried out by dissolving PLM in dichloromethane (CH_2Cl_2), which was then precipitated in excess methanol. This process was repeated twice to remove the residue of monomers. The benzyl protective groups were removed by the catalytic hydrogenolysis using $Pd(OH)_2/C$ as the catalyst. Briefly, PLM (2 g) was dissolved in 60 ml of chloroform ($CHCl_3$) first and then 0.6 g of $Pd(OH)_2/C$ (10%) in 20 ml of ethyl acetate was added into the polymer solution. After being evacuated and filled with hydrogen, the solution was stirred at room temperature for 24 h. The catalyst was filtered and the solution was precipitated into excess methanol. The obtained polymer was then redissolved in CH_2Cl_2 and the solution was centrifuged at 13,000 rpm (11 kg) for 1 h at −5 °C to further remove the catalyst residue. Immobilization of heparin was carried out through the activation of heparin sodium salt (187 unit mg^{-1}, Sigma) with 1-(3-dimethylaminopropyl)-3-ethylcarbodiimide hydrochloride (EDC·HCl, Sigma, St. Louis, MO) in a sodium citrate buffer solution (pH 4.7) at 4 °C for 5 h, followed by surface conjugation with the carboxyl acid groups of the deprotected copolymer films at 4 °C for 24 h. After the immobilization reaction, polymer films were washed with PBS and 0.1% Triton X-100 aqueous solution, and then subsequently rinsed with distilled water in an ultrasonic cleaner until there was no residue of non-immobilized heparin. After drying in vacuum at room temperature, heparinized copolymer films were recovered. PLM copolymers (Co90, Co80 and Co70) with three LA contents (90%, 80% and 70%), were used to achieve different heparinized copolymers: Hep-Co90, Hep-Co80 and Hep-Co70, respectively.

A standard linear relationship for quantifying heparin was obtained by the toluidine blue colorimetric method [22], described as follows. Three milliliters of toluidine blue solution (0.05 g of toluidine blue in 1 l of 0.01 N HCl containing 0.2% NaCl) was pipetted into each of four test tubes. Then 2 ml of standard solution with a varied concentration of heparin was added to the toluidine blue solution. After extraction using 3 ml of hexane for 30 min, the aqueous layers of the solution were sampled. The absorbance at 631 nm was measured and the amount of heparin immobilized on the polymer film was then calculated using the calibration curve constructed earlier.

2.2. Characterizations of heparin-immobilized polymers

Tensile tests were performed at room temperature using an Instron dynamometer (model 3366) on strips (100 × 10 mm, length × width) cut from the cast polymer films at a cross-head speed of 1 mm min^{-1}. The inherent viscosities of the dilute solutions of the heparinized polymers in $CHCl_3$ were determined using a Ubbelohde viscometer at 28 °C. A static contact angle system (Kruss, Model DSA16) with water as the liquid phase was used to test the hydrophilicity of the polymer surface. Approximately 1 μl of water (pH 7.0) was injected onto the polymer surface. Contact angle measurement was performed after a static time of 30 s and a tangent method was applied to obtain the contact angles in degrees. For each sample, three specimens were used and six data points were taken for calculating the average and standard deviation.

2.3. In vitro hemocompatibility

In vitro hemocompatibility of the heparinized copolymers was evaluated in the aspects of platelet adhesion, protein adsorption, full human plasma recalcification time and thromboplastin time. Heparinized copolymer films were prepared by casting their CH_2Cl_2 solutions (5% w/v) on glass templates. After 24 h of solvent evaporation, the films were further dried under reduced pressure at room temperature until a constant weight was reached. Blood was drawn from healthy volunteers and mixed with a 3.8 wt.% solution of sodium citrate at a dilution ratio of 9:1 (blood:sodium citrate solution). Platelet-rich plasma (PRP) and platelet-poor

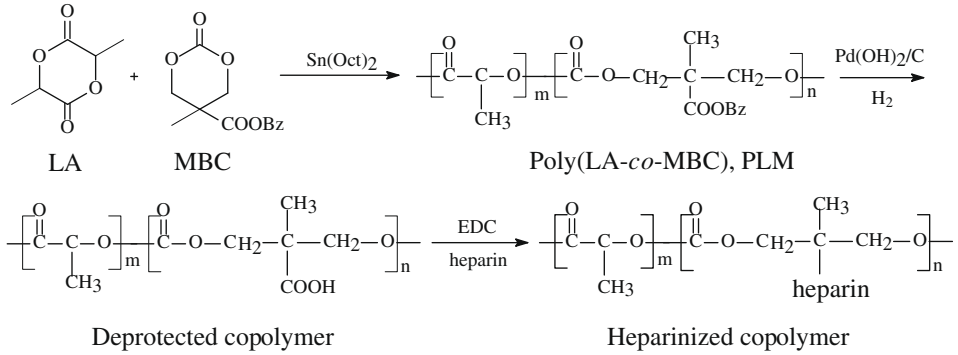

Fig. 1. Synthesis of poly(LA-*co*-MBC) (PLM) and heparinized copolymer.

Please cite this article in press as: Gong F et al. Heparin-immobilized polymers as non-inflammatory and non-thrombogenic coating materials for arsenic trioxide eluting stents. Acta Biomater (2009), doi:10.1016/j.actbio.2009.07.013

plasma (PPP) were obtained by centrifuging citrated blood at 1200 rpm (100 g) for 5 min and at 3000 rpm (600 g) for 10 min, respectively.

The experimental procedure for determining platelet adhesion is given as follows. Polymer films (0.2 g) were weighed in 5 ml syringes and equilibrated with 2 ml of phosphate-buffered saline (PBS, pH 7.4, 0.15 M) for 12 h. After that, the buffer was removed and 2 ml of PRP was introduced into the syringes. The syringes were rotated in a shaking incubator at 37 °C for 5, 10, 15, 20, 25, 30, 60, 90 and 120 min. At each time point, the syringes were quickly removed from the shaking incubator and the depleted platelets in the PRP were counted immediately using a hemacytometer. The amount of platelets adhered to the specimen was calculated by subtracting the number of unadhered platelets from the number of diluted platelets initially incubated.

A bicinchoninic acid protein assay (MicroBCA) was performed to determine the total amount of protein adsorbed onto the polymer surface from PPP [23]. Prewetted polymer films (12 × 0.3 mm, diameter × thickness) were incubated in 24-well plates containing 2 ml of PPP at 37 °C for 5, 15, 30, 60 and 120 min, respectively. Each sample was then rinsed with PBS and incubated with 2 ml of 1% sodium dodecyl sulfate (SDS) solution for 1 h. The SDS solution was collected in a plastic vial, and fresh SDS solution was added to the wells for another 1 h. This procedure was repeated twice, with all the SDS solutions being collected in plastic vials. The concentrations of protein in the collected SDS solutions were determined on a microplate reader using a MicroBCA protein assay kit (Shanghai Xinhang, 250 ml) [24,25]. The amount of irreversibly adsorbed proteins on the polymer surfaces was then calculated.

Full human plasma recalcification time and thromboplastin time were measured as follows. About 0.1 ml of PPP was introduced onto the polymer surfaces and incubated at 37 °C under static conditions for 10 min. Next, 0.1 ml of a 0.025 M aqueous solution of $CaCl_2$ was added to the PPP. The plasma solution was monitored for clotting by manually dipping a stainless steel wire hook coated with silicone into the plasma solution to detect fibrin threads. The clotting time was recorded at the first sign of fibrin formation on the hook. At least three recalcification experiments were carried out on each polymer surface. The full human plasma thromboplastin time of the polymer films were measured on an automatic Sysmex CA-1500 coagulation analyzer using Dade Behring Actin, Dade Behring Thromburel's and Dade Behring Test-Thrombin reagents. The paired *t*-test was used and the significance level was set as $p < 0.03$.

2.4. Preparation and surface morphology of polymer-coated stents and As_2O_3-eluting stents

Bare metal stents (3.0 × 17 mm, diameter × length, Beijing Amsinomed Medical Company, China) were washed with ethanol and isopropanol, then dried in vacuum at room temperature for 1 day. Heparinized copolymer films were dissolved in CH_2Cl_2 at 0.1 wt.% and sprayed onto the surface of each BMS, then dried in vacuum at room temperature for 3 days. The quantity of polymer was 60 ± 5 μg per stent. Because of the solubility of As_2O_3 in water, a three-layer method was developed for the preparation of As_2O_3-eluting stents. Hep-Co90/CH_2Cl_2 solution (0.1 wt.%), As_2O_3 aqueous solution (1 wt.%) and Hep-Co90/CH_2Cl_2 solution (0.1 wt.%) were sprayed sequentially onto the stent surface to prepare the basecoat, drug layer and topcoat, respectively. The quantity of polymer in the basecoat and topcoat was 20 ± 3 and 40 ± 5 μg, respectively. The quantity of As_2O_3 was 40 ± 5 μg per stent, or 2.35 μg mm^{-1} (mass per length). The surface morphology of the polymer-coated stents and As_2O_3-eluting stents was examined using scanning electron microscopy (SEM; JSM-6360LV, JOEL) before balloon expansion. The stents were mounted onto an angioplasty balloon (3.0 mm) and the balloon was inflated to a maximum pressure of 18 atm for 30 s, deflated and withdrawn slowly. The post-expansion stents were also examined using SEM.

2.5. In vitro hydrolytic degradation and heparin release profile of the polymer-coated stents

Polymer-coated stents were immersed in 10 ml PBS (pH 7.4) at 37 °C in a shaking incubator for up to 4 months. The PBS solution was renewed every three days. In vitro hydrolysis was determined by measuring the weight loss of the coating every month ($n = 5$ for each time point).

The in vitro heparin release profile from the coated stents was obtained as follows. Heparinized-copolymer-coated stents were placed in syringes and equilibrated with 10 ml of PBS (pH 7.4). These syringes were then tapped to remove air bubbles, sealed and rotated in a shaking incubator at 37 °C for 1, 2, 3 and 4 months. At each time point ($n = 3$ for each sample), syringes were taken away from the shaking incubator and the heparin in PBS was measured by the toluidine blue method described in Section 2.1. Then the heparin remained in the stent coating was calculated.

2.6. As_2O_3 release profile from the polymer-coated stents

The in vitro release profile of As_2O_3 from the stents was evaluated by immersing each stent in a 20 ml syringe equilibrated with 20 ml of PBS (pH 7.4, 0.15 M) at 37 °C in a shaking incubator ($n = 5$ stents per time point). At each time point, the syringes were quickly removed from the incubator and the concentration of As_2O_3 in PBS was measured using the hydride generation reaction interfaced with atomic fluorescence spectrometry assay [20].

2.7. Animal implantations

A porcine coronary artery model was used to evaluate the biocompatibility and functionality of BMSs, polymer-coated stents and As_2O_3-eluting stents. Sixty male pigs, weighing 20–30 kg each, were obtained from the Shanghai Animal Administration Center. All animal studies were approved by the Animal Care and Use Committee of Fudan University and were in compliance with the "Guide for the Care and Use of Laboratory Animals" published by the National Academy Press (NIH Publication No. 85–23, revised in 1996). Before implantation, the stents were sterilized with ethylene oxide and kept under aseptic conditions. All stents were divided into six groups, with 24 pieces per group: BMSs, stents coated with Co90, Hep-Co90, Hep-Co80, and Hep-Co70, and As_2O_3-eluting stents using Hep-Co90 as the drug vehicle. For each group, three stents were used to analyze the apoptosis of vessel smooth muscle cells (VSMCs). Animals were kept under the same conditions and administered 300 mg of aspirin per day in their feed for 3 days before implantation. For each pig, two or three stents were randomly implanted into the left anterior descending artery (LAD), right coronary artery (RCA) and left circumflex artery (LCX) using online quantitative coronary angiography. When the LCX was too small for stent implantation, only the LAD and RCA received stents. On the day of stent implantation, iliac artery access was achieved under general anesthesia and a 7F sheath was inserted. After the administration of 10,000 units of heparin, the target coronary artery was engaged using standard 7F guide catheters and the control angiograms of the both coronary arteries were performed using non-ionic contrast agent in two orthogonal views. The stent was deployed by inflating the balloon (3.0 mm) to a nominal pressure at the site of injury caused by overstretching, and the resultant stent-to-artery ratio was 1.3:1. Repeated angiograms were obtained immediately after the stent implantation, then all the equipment was removed and the iliac artery was ligated.

Please cite this article in press as: Gong F et al. Heparin-immobilized polymers as non-inflammatory and non-thrombogenic coating materials for arsenic trioxide eluting stents. Acta Biomater (2009), doi:10.1016/j.actbio.2009.07.013

After 1, 3 and 6 months, animals were anesthetized for angiography to confirm the patency of the coronary artery. Thereafter, a lethal amount of potassium chloride was injected to induce euthanasia. Vessels with stents at 1, 3 and 6 months ($n = 7$ for each group) after implantation were cut into five pieces, each about 3 mm long, fixed in 10 ml of buffered formalin and embedded in methacrylate. The cross-sections from proximal, distal and medial pieces were obtained using a section cutter (Leica SP1010, Germany) and stained with hematoxylin and eosin for measuring vessel area and performing histological analysis with Leica Qvin V3 software. Sections from the other pieces were cut open lengthwise and fixed with 1% osmium tetroxide for SEM photographing. To evaluate the in vivo degradation of the stent coatings, the stent surface was also observed using SEM after the blood vessel tissue was carefully peeled off from the stent surface under a microscope without causing destruction of the coatings.

2.8. Histological analysis of neointimal hyperplasia

The areas enclosed by external elastic lamina (EEL, mm^2) and internal elastic lamina (IEL, mm^2) and the lumen area (LA, mm^2) were measured. Neointimal area (NA, mm^2) was calculated as follows: NA = IEL−LA. The percent neointimal stenosis was calculated using the equation: % stenosis = NA/IEL × 100. Mean neointimal thickness was calculated using the equation: mean neointimal thickness = $\sqrt{IEL/\pi} - \sqrt{LA/\pi}$ [20].

2.9. CD3 immunostaining

The sections were deparaffinized, heated at 95 °C for 30 min in antigen retrieval solution, fixed in 0.3% hydrogen peroxide for 30 min and then air dried. Nonspecific binding was blocked by a 30 min incubation in normal horse serum (10 vol.%, 0.1% Triton X-100, 0.1 M PBS, pH 7.4). The slide was then incubated in the CD3 primary antibody (1:100, 0.1% Triton X-100, 0.1 M PBS) (R&D systems, Minneapolis, MN, USA) overnight at 4 °C. After three washes in PBS, the slides were again blocked in normal horse serum as described above and exposed to the horseradish peroxidase-conjugated secondary antibody (1:400, 0.1% Triton X-100, 0.1 M PBS) (Beyotime, China), followed by the addition of 3,3′-diaminobenzidine tetrahydrochloride (DAB) solution. The total tissue area of the immunostained sections of each specimen was outlined manually and measured in mm^2. The tissue areas of the immunostained sections occupied by CD3-positive cells were measured automatically using greyscale detection with a fixed threshold and the ratios of immunopositive areas were calculated as percentages of the total tissue area.

2.10. Apoptosis of VSMCs

Apoptosis of VSMCs was evaluated by the TUNEL (terminal deoxynucleotidyl transferase-mediated dUTP nick-end labeling) assay using DAB as the chromogen (Boehringer Mannheim Inc., Germany) 7 days post-implantation. The stented vessels were fixed in 10% buffered formalin and embedded in paraffin. Cross-sections from the proximal end were washed and counterstained with hematoxylin. This method identifies apoptotically degraded DNA. Only cells with distinct nuclear staining were considered. VSMCs in intimal and media were counted in three cross-sections for each arterial specimen. The number of TUNEL-positive VSMCs was expressed as a percentage of the total number of VSMCs.

2.11. Statistical analysis

Numerical data are presented as means ± standard error of the mean. Continuous variables were compared by analysis of variance (t-test with Bonferroni correction), and categorical variables were compared by χ^2-test. A p value of less than or equal to 0.05 was considered as significantly different.

3. Results and discussion

3.1. Synthesis and structural characterizations of heparinized copolymers

As listed in Table 1, three heparinized copolymers, Hep-Co90, Hep-Co80 and Hep-Co70 were characterized using FTIR (Nicolet MagnaTR550), ^{1}H NMR (Bruker DRX-500) and elemental analysis (vario EL III). FTIR (KBr): 3310 cm^{-1} (ν_{O-H}), 2960–2980 cm^{-1} (ν_{C-H}), 1760 cm^{-1} ($\nu_{C=O}$), 1630 cm^{-1} (δ_{N-H}), 895 cm^{-1} (ν_{S-O}). ^{1}H NMR ($CDCl_3$): δ = 1.37 (t, C–CH_3), 1.60 (s, O–CH–CH_3), 4.50 (m, O–CH_2), 5.15 (m, CH_2–Bz), 5.21 (m, O–CH–CH_3), 7.26 (s, –C_6H_5). Sulfur content is 1.09%, 1.28% and 1.45% for Hep-Co90, Hep-Co80 and Hep-Co70, respectively. The physical properties of the heparinized copolymers are also listed in Table 1. Intrinsic viscosity decreases with decreasing LA content in the copolymers possibly because of the lower molecular weight resulting from the lower reactivity of the MBC monomer compared with that of LA. Consequently, Young's modulus and strength at break decrease from 373 and 42 MPa for Hep-Co90 to 244 and 29 MPa for Hep-Co70, respectively. Meanwhile, the elongation at break increases from 160% to 290%, indicating that the heparinized copolymer is stiffer when the LA content is higher. The deprotection ratio of the benzyl groups is closely related to the molecular weight of the copolymer because of steric hindrance. The deprotection ratio determined using ^{1}H NMR is only 24% in Hep-Co90. It increases to 42% in Hep-Co70 and results in a higher degree of heparin immobilization, as indicated by the surface heparin content in Table 1. The contact angle of water on the copolymer surface decreases from 82.7° for Hep-Co90 to 73.2° for Hep-Co70. It suggests that a less hydrophobic surface can be achieved when the LA content is lower and the surface heparin content is higher.

3.2. Surface morphology examination and balloon expansion tests

Surface topography is crucial for the in vivo performance of DESs [26,27]. Webbings and bridges between the struts may cause inflammation and VSMC proliferation, consequently resulting in higher rates of thrombosis and restenosis. Fig. 2 shows the SEM images of Hep-Co90-coated stents and As_2O_3-eluting stents before and after expansion. Stents coated with Co90, Hep-Co80 and Hep-Co70 are not presented in Fig. 2 because they are similar to Hep-Co90-coated stents. The coatings in Fig. 2A and B are uniform and smooth before the dilation using an angioplasty balloon

Table 1
Physical properties of the polymers in this study.

Sample	LA content (mol%)	[η] (dL/g)	Young's modulus (MPa)	Strength at break (MPa)	Elongation at break (%)	Deprotection ratio (%)	Surface heparin content (μg/cm^2)	Contact angle (°)
Hep-Co90	90	2.14	373 ± 29	42 ± 7	160 ± 18	24	2.57	82.7
Hep-Co80	80	1.88	304 ± 22	37 ± 7	220 ± 23	31	4.96	76.3
Hep-Co70	70	1.10	244 ± 27	29 ± 6	290 ± 28	42	6.33	73.2

Please cite this article in press as: Gong F et al. Heparin-immobilized polymers as non-inflammatory and non-thrombogenic coating materials for arsenic trioxide eluting stents. Acta Biomater (2009), doi:10.1016/j.actbio.2009.07.013

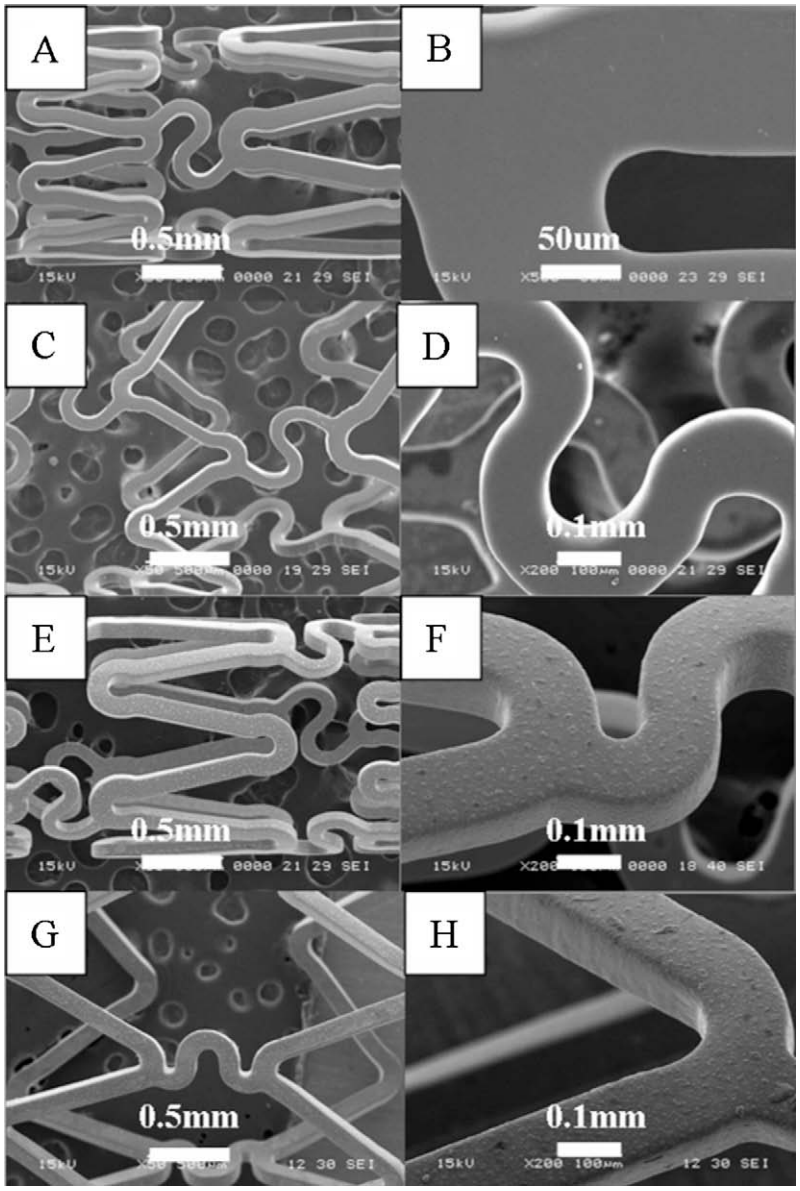

Fig. 2. SEM images of Hep-Co90-coated stents (A–D) and As_2O_3-eluting stents (E–H). A (50×), B (500×), E (50×) and F (200×) are pre-expansion images. C (50×), D (200×), G (50×) and H (200×) are post-dilation images. The scale bars in A, C, E and G are 0.5 mm. The scale bar in B is 50 μm. The scale bars in D, F and H are 0.1 mm.

catheter. No delamination or destruction of the coating on the stent can be observed in Fig. 2C and D after expansion, indicating that the polymer coating has sufficient flexibility to allow balloon expansion of the stent without cracking or peeling from the struts. For As_2O_3-eluting stents, As_2O_3 aqueous solution was sprayed onto the surface of the polymer basecoat, dried in vacuum and covered by the polymer topcoat. It can be clearly seen in Fig. 2E and F that As_2O_3 crystals disperse between the basecoat and topcoat. After expansion (Fig. 2G and H), still no destruction of the coating can be found, indicating that the introduction of the drug does not impair the integrity of the polymer coating.

3.3. Hemocompatibility evaluation

Stent coating is important in determining vascular responses, such as the event cascade beginning with platelet and protein deposition at the struts, followed by VSMC migration and eventually neointimal hyperplasia [28]. Fig. 3 shows the results of the in vitro blood contact test on the surfaces of Co90 and three heparinized copolymers. All the heparinized copolymers have lower platelet adhesion compared with the Co90 control group. Fibrinogen plays an important role in platelet-surface attachment because platelet GPIIb/IIIa can only recognize the bound fibrinogen, having undergone appropriate conformational changes [29]. This phenomenon might contribute to the decreased platelet adhesion on the heparinized copolymers together with the well-known electrical repulsion between the negatively charged heparin and platelets. The heparinized copolymers in Fig. 3B have ~50% lower protein adsorption than Co90. The polymer surface's capability of adsorbing protein from plasma is regulated by ionic, hydrophilic and/or hydrophobic interactions. The conjugation of heparin with copolymer not only improves copolymer hydrophilicity but also increases the steric hindrance between the protein and the copolymer surface, both of which are believed to reduce the capability of adsorbing protein from plasma.

Plasma recalcification time and thromboplastin time are two parameters for evaluating the in vitro hemocompatibility of materials [23,26]. When Ca^{2+} (factor IV) is complemented to the antico-

Please cite this article in press as: Gong F et al. Heparin-immobilized polymers as non-inflammatory and non-thrombogenic coating materials for arsenic trioxide eluting stents. Acta Biomater (2009), doi:10.1016/j.actbio.2009.07.013

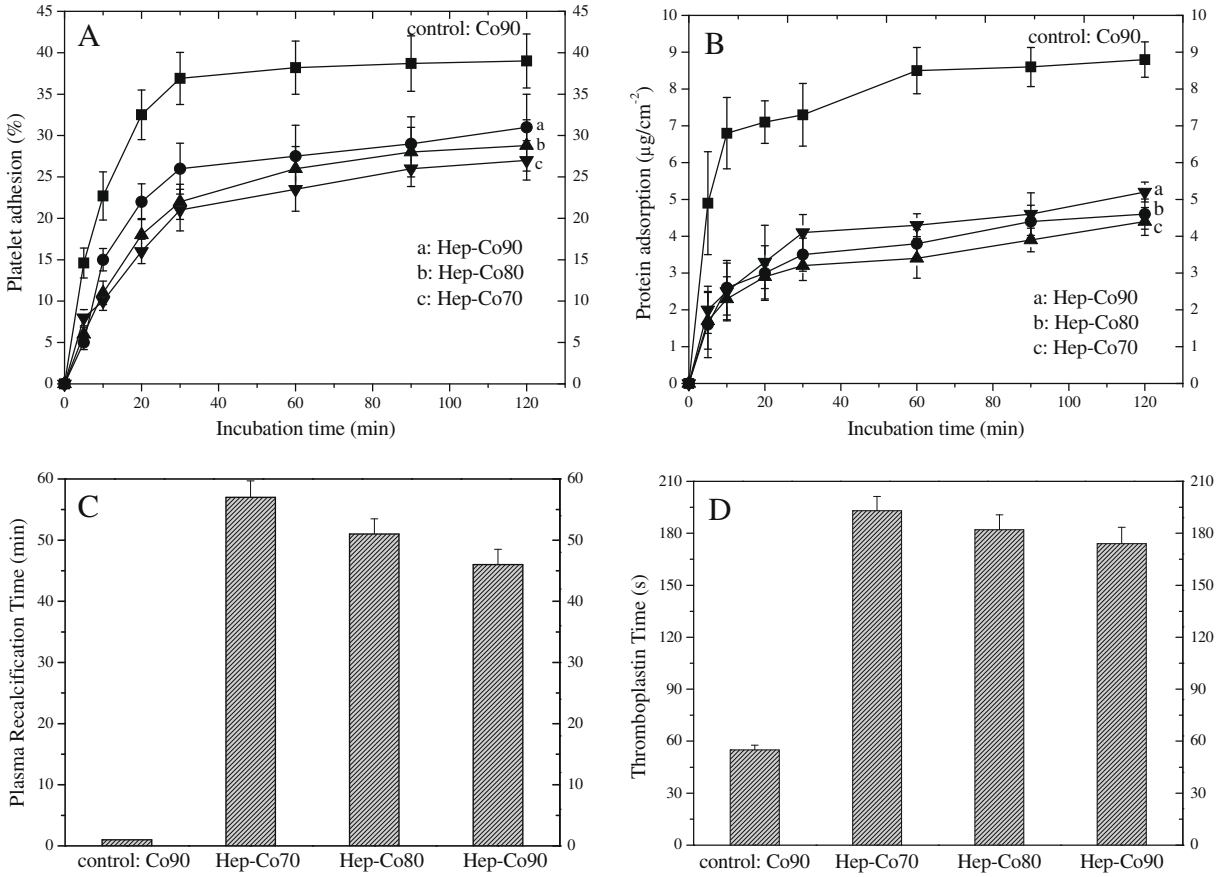

Fig. 3. Platelet adhesion (A), protein adsorption (B), plasma recalcification time (C) and thromboplastin time (D) on different polymer films.

agulated PPP, prothrombin (factor II) will be activated by the endogenous blood coagulation system and converted to thrombin [30]. Thrombin, in turn, will start the formation of insoluble fibrin from fibrinogen. Fig. 3C shows the plasma recalcification time on different polymer surfaces, whereas the value on the Co90 surface is only about 1 min. After heparinizing the copolymers, the plasma recalcification time increases to around 46, 51 and 57 min for Hep-Co90, Hep-Co80 and Hep-Co70, respectively. As proposed in the literature [31], some heparin molecules attached on the stent surface have an epsilon-shaped antithrombin III binding site where circulating antithrombin can become incorporated and catalyze the inhibition of activated coagulation factors, e.g. thrombin. The resultant inactive antithrombin/thrombin complex is then released into the bloodstream to enable the active site on the heparin to repeat the interaction with antithrombin III and create more antithrombin/thrombin complex [31]. The plasma recalcification time increases with the increase in the amount of immobilized heparin. The thromboplastin time for different polymers (Fig. 3D) shows the same trend. The above results indicate that the anticoagulant activity of the heparin molecules remained after surface immobilization.

3.4. Hydrolytic degradation and heparin release profile of the coated stents

For DESs coated with biodegradable polymers, the degradation properties of the coatings greatly influence their in vivo performance [7,32]. The hydrolytic degradation of the stent coatings in 0.001 M PBS aqueous solution (pH 7.4) was evaluated. Fig. 4C shows a general trend of faster weight loss for the heparinized copolymer coatings than for Co90. This trend may be attributed to the improved hydrophilicity by heparin conjugation. With increasing MBC content, a higher hydrolytical rate can be observed because of the higher content of hydrophilic carboxyl acid groups on the side chains of the deprotected polymers and the relatively lower molecular weight. The total degradation time of these four stent coatings in PBS was between 3 and 4 months.

Fig. 4A shows a time series of SEM images of Hep-Co90-coated stents before and after immersion in PBS for 1, 2 and 3 months. After a 1 month incubation, the initially smooth surface became porous (Fig. 4A1). Further development of the inner phase could be observed after 2 months (Fig. 4A2). The pore size and density increased with time of incubation up to 3 months (Fig. 4A3). The film surface became irregular, rough and porous progressively. After 3 months of incubation, little residual polymer coating could be observed on the stent surface and the weight loss of the coatings was above 85%.

Although the examination of the surface morphological changes of polymer-coated stents using SEM could not elucidate the degradation mechanism, it supplied useful information about the in vivo degradation properties. Fig. 4B shows the morphological changes of the Hep-Co90 coating on the stents implanted in porcine coronary arteries for 1, 2 and 3 months. After 1 month, the coating surface had become very rough; small fragments of the coating can be observed in Fig. 4B1. The polymer coating can still be observed after 2 months (Fig. 4B2). After 3 months, little residual polymer coating was present and the stent surface had become smooth again, as shown in Fig. 4B3. The stent surface was extracted with CH_2Cl_2 for FTIR analysis. The FTIR spectrum was >98% consistent with that of cell cytoplasm, also suggesting that there was little residual polymer coating after degradation in vivo for 3 months. Stents coated with Co90, Hep-Co80 and Hep-Co70 had similar results in degradation and are therefore, omitted from Fig. 4 for simplification.

Please cite this article in press as: Gong F et al. Heparin-immobilized polymers as non-inflammatory and non-thrombogenic coating materials for arsenic trioxide eluting stents. Acta Biomater (2009), doi:10.1016/j.actbio.2009.07.013

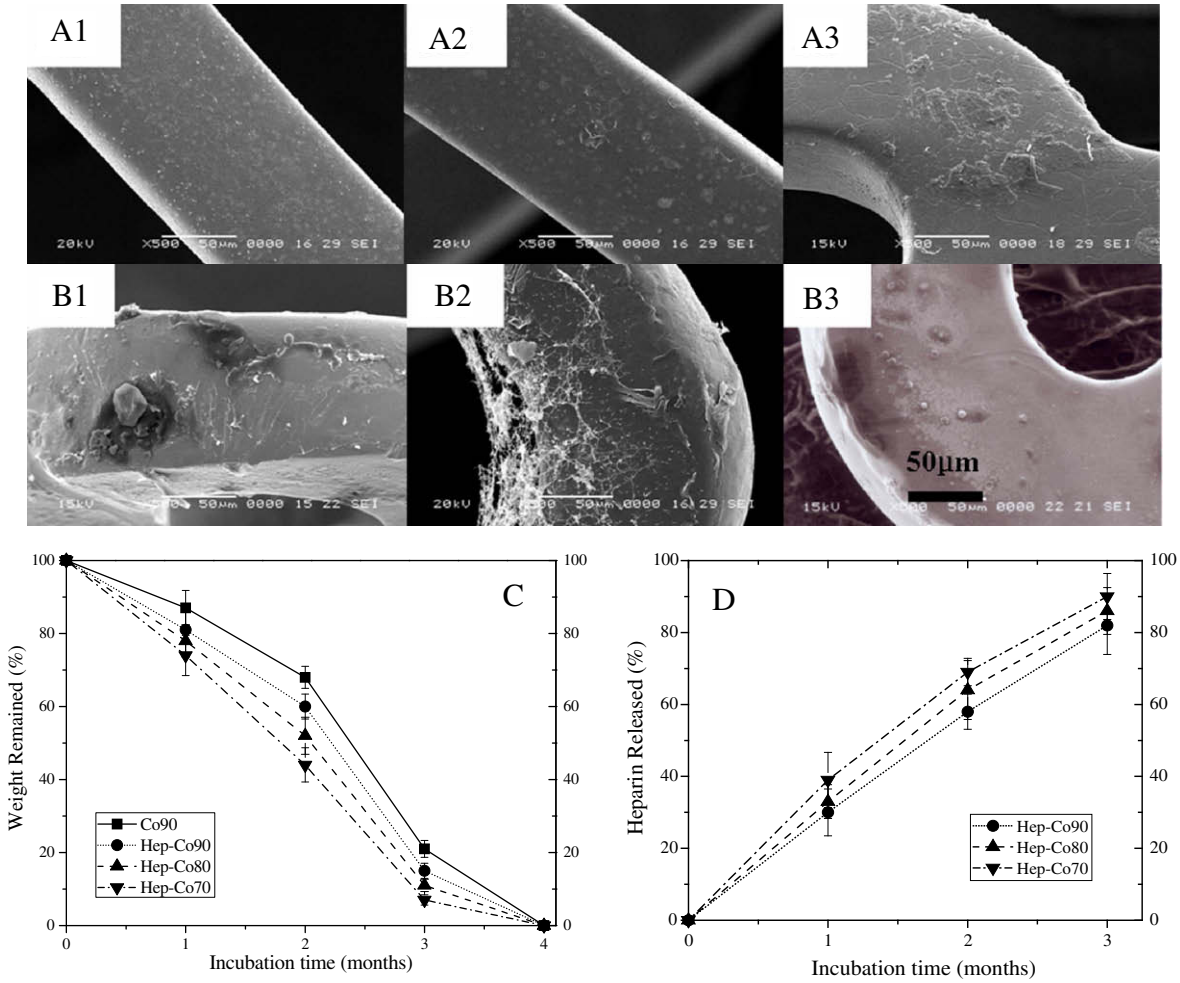

Fig. 4. SEM images of Hep-Co90-coated stents after degradation in vitro (A) and in vivo (B) for 1 (A1 and B1), 2 (A2 and B2) and 3 months (A3 and B3). The scale bar in B3 is 50 μm and is applicable for both (A and B). (C) Weight loss of the stent coatings in PBS; (D) heparin released from the stent coatings in PBS.

Based on the standard absorbance curve (not shown), in vitro release profiles of heparin from the heparinized-copolymer-coated stents were obtained, as shown in Fig. 4D. All the copolymer coatings exhibited similar sustained-release profiles of conjugated heparin within 4 months despite their differences in molecular weight and the content of conjugated heparin. All the conjugated heparin reached a cumulative release plateau of over 95% after 4 months of incubation in PBS, which is consistent with their in vitro hydrolytic degradation properties.

3.5. Endothelialization of stented arteries

The endothelialization of stented arteries ($n = 3$ for each group) was examined using SEM at 1 month after stent implantation. In most reports, there was no significant difference in extensive endothelialization between DESs and BMSs at 28 days post-implantation in both rabbit and porcine models [33,34]. As shown in Fig. 5, the arteries treated with BMSs or Hep-Co90-coated stents were fully endothelialized, the lumen surface of the vessel wall and the stent struts being covered by confluent endothelial cells. Although an As_2O_3-eluting stent was reported to mildly delay endothelialization in a rabbit iliac artery injury model [20], complete endothelialization with a cobblestone structure covering the smooth muscle layer could be observed in the present study when the stents were implanted in porcine coronary arteries. The fast-release profile of this anti-proliferative agent may contribute to the rapid endothelialization of As_2O_3-eluting stents. As shown in Fig. 6, As_2O_3 could be released completely from the polymer coating 7 days after implantation. In contrast, in some Hep-Co70-coated stents, the surfaces were not fully covered by endothelial cells – possibly due to a severe inflammatory reaction. In sirolimus- and paclitaxel-eluting stents, the proliferation of smooth muscle cells, which causes neointimal thickening, was suppressed, while the endothelialization of the injured blood vessel might be delayed by their sustained-release profiles [35–37]. A higher thrombosis rate will occur if the stent surface is not covered by endothelial cells. Thus the anti-platelet treatment needs to be maintained for approximately 6–18 months after the implantation of DESs. Anti-platelet agents, however, can generate side effects. In the current clinical trials of As_2O_3-eluting stents in China, anti-platelet treatment does not need to last for longer than 3 months because of the fast-release profile and quick endothelialization. No in-stent thrombosis has been observed up to 9 months for all the patients (more than 100), indicating the biocompatibility and high potentials of As_2O_3-eluting stents. In other words, the fast-release profile of As_2O_3 causes less delay in endothelialization; consequently thrombosis will not form and anti-platelet treatment is unnecessary for a longer period.

3.6. Histological analysis and morphometric evaluations

The heparinized copolymers synthesized in the present study are expected to be non-inflammatory and non-thrombogenic coating materials for As_2O_3 elution. As demonstrated in Fig. 7, the

Please cite this article in press as: Gong F et al. Heparin-immobilized polymers as non-inflammatory and non-thrombogenic coating materials for arsenic trioxide eluting stents. Acta Biomater (2009), doi:10.1016/j.actbio.2009.07.013

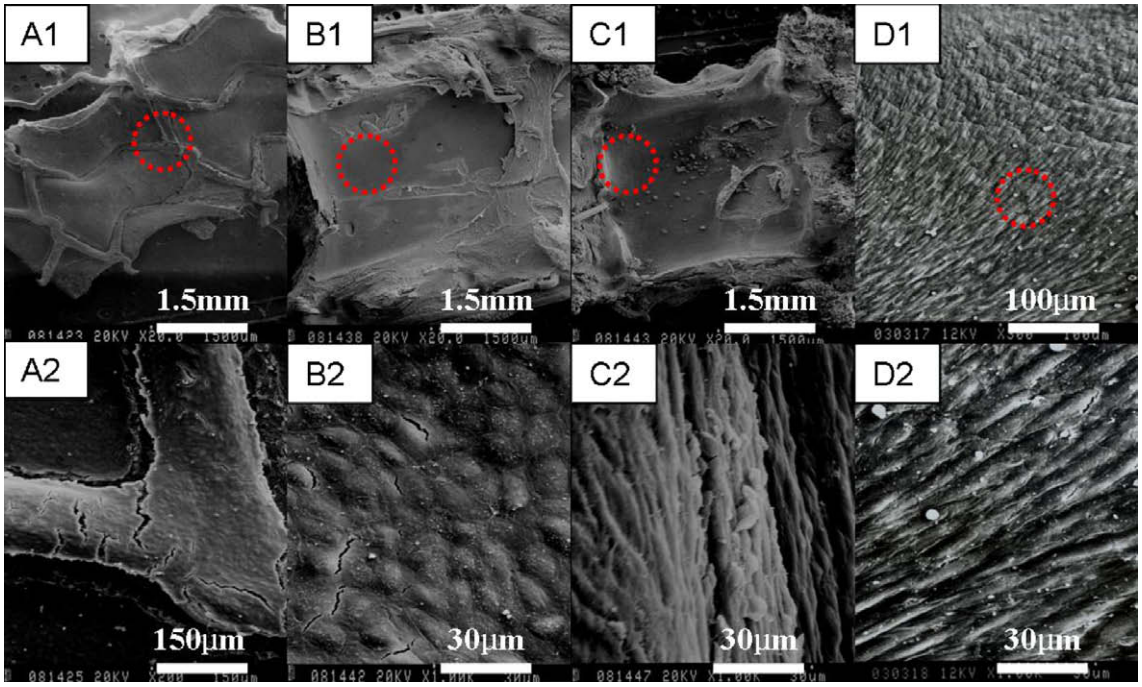

Fig. 5. SEM images of the porcine coronary arteries 1 month after stent implantation. The bottom images are magnified views of the dotted areas in the top images. A BMS (A), Hep-Co90-coated stent (B) and As_2O_3-eluting stent (D) were fully covered with endothelial cells with a cobblestone structure. The Hep-Co70-coated stent (C) were not covered by endothelial cells. The scale bars in A1, B1 and C1 are 150 μm. The scale bar in D1 is 100 μm. The scale bar in A2 is 150 μm. The scale bars in B2, C2 and D2 are 30 μm. The stented blood vessel was fixed with 1% osmium tetroxide.

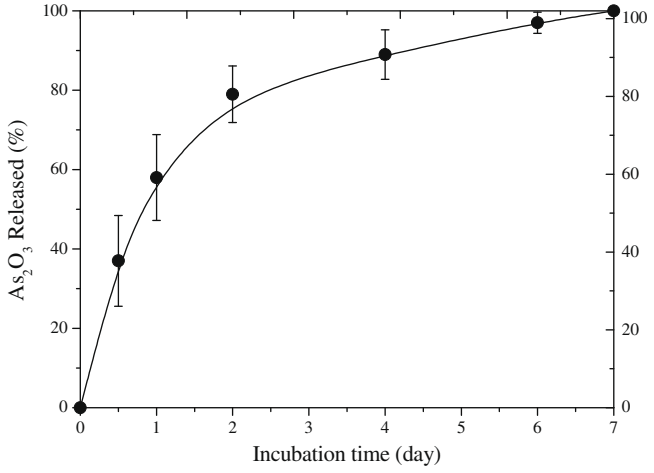

Fig. 6. In vitro drug release from the As_2O_3-eluting stents.

effects of the copolymer coatings and As_2O_3 on restenosis and inflammation were evaluated in a porcine coronary artery injury model using BMS as the control group. The morphometric data obtained from the arteries treated with different stents in Fig. 7 are shown in Fig. 8. Angiograms of the coronary arteries 1, 3 and 6 months after the implantation of As_2O_3-eluting stents are illustrated in Fig. 9. No distinctive vessel narrowing and remodeling effect on the surrounding tissue could be observed after the coronary arteries were implanted with As_2O_3-eluting stents. As_2O_3 had a remarkable effect on reducing neointimal hyperplasia. No in-stent thrombosis appeared in any stenting groups in the present study, although late-stage thrombosis in stents with biostable polymer coatings usually happens beyond the six-month timeframe of our animal study. Meanwhile, no As_2O_3 could be detected in the serum, heart, liver, kidney or stented blood vessel at day 7 post-implantation. A complete blood cell count showed similar results for white blood cell count, platelet count and hematocrit among all groups.

As presented in Fig. 8B and C, neointimal area and thickness at 1 month post-implantation were 2.4 ± 0.4 mm^2, 0.29 ± 0.04 mm; 3.3 ± 0.4 mm^2, 0.42 ± 0.04 mm; 2.3 ± 0.1 mm^2, 0.27 ± 0.02 mm; 3.3 ± 0.3 mm^2, 0.42 ± 0.04 mm; 4.3 ± 0.1 mm^2, 0.57 ± 0.02 mm; and 2.1 ± 0.2 mm^2, 0.22 ± 0.02 mm for BMSs, stents coated with Co90, Hep-Co90, Hep-Co80 and Hep-Co70, and As_2O_3-eluting stents, respectively. Although heparin immobilization is expected to improve the biocompatibility of polymer coatings [38–42], distinctive vessel narrowing and a remodeling effect on the surrounding tissue induced by the severe inflammatory response could be observed in the stents coated with Co90, Hep-Co80 and Hep-Co70, as shown in Fig. 7B, D and E, respectively. Lymphohistiocytic reactions could be also seen in these polymer coatings. The adverse reactions found in the stents coated with Hep-Co80 and Hep-Co70 can be attributed to their relatively higher degradation rates resulting from their lower molecular weights and better hydrophilicity compared with Hep-Co90. Better hydrophilicity may improve the biocompatibility of non-biodegradable coating materials [43]. For the biodegradable coating materials used in DESs, however, the rapid water uptake in the heparinized copolymer with a lower molecular weight leads to an accelerated rate of ester hydrolysis compared with the copolymers with higher molecular weights and consequently stimulates additional inflammation and neointimal hyperplasia [44].

In contrast to the severe neointimal response induced by the Co90, Hep-Co80 and Hep-Co70 coatings exemplified in Fig. 7H and I, only a mild inflammatory response of fibromuscular proliferation could be observed around the struts of Hep-Co90-coated stents (Fig. 7G) when implanted in porcine coronary arteries. The stented blood vessels were also stained using a standard protocol for hematoxylin and eosin. An immunohistochemistry procedure was used to stain the antigen CD3, a marker of T lymphocytic cells. The ratios of CD3-positive cell for BMSs, Co90, Hep-Co90,

Please cite this article in press as: Gong F et al. Heparin-immobilized polymers as non-inflammatory and non-thrombogenic coating materials for arsenic trioxide eluting stents. Acta Biomater (2009), doi:10.1016/j.actbio.2009.07.013

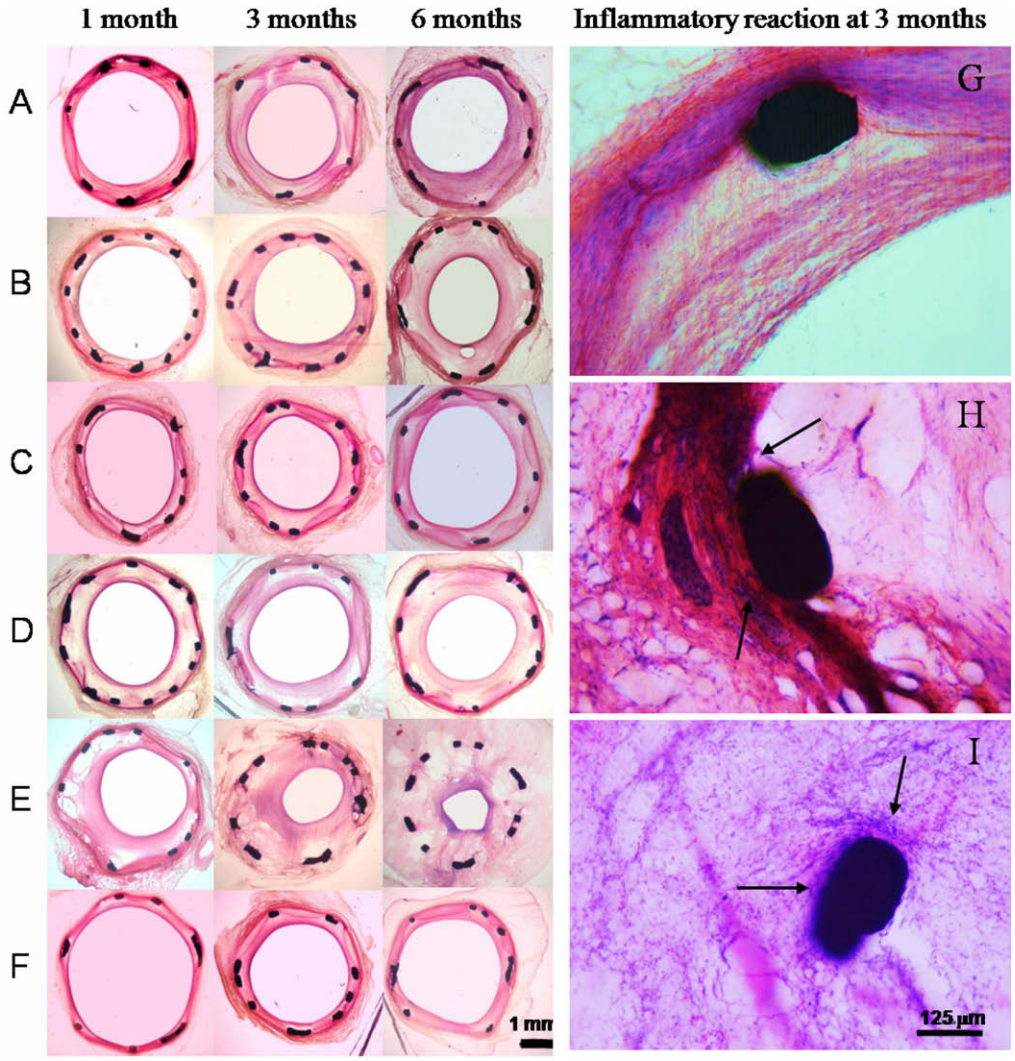

Fig. 7. Photomicrographs of the blood vessel segments (A–F) and the inflammatory reaction for different polymer-coated stents (G–I). (A) BMSs; (B–F) stents coated with Co90, Hep-Co90, Hep-Co80 and Hep-Co70, and As_2O_3-eluting stents, respectively. The scale bar of 1 mm in (F) (6 months) is also applicable for (A–E). (G) Stent coated with Hep-Co90 showing only a mild inflammatory response of fibromuscular type; (H and I) stents coated with Hep-Co80 and Hep-Co70, respectively. The scale bar of 125 μm in (I) is also applicable for (G) and (H). In (H and I) a severe inflammatory reaction of lymphohistiocytic type can be observed and much of the strut interface surface is masked by inflammatory cells (arrows).

Hep-Co80, Hep-Co70 and As_2O_3-eluting stents were 20.6 ± 4.1%, 26.7 ± 6.4%, 19.8 ± 4.5%, 28.6 ± 6.1%, 31.4 ± 7.3% and 6.7 ± 2.9%, respectively. The above results indicate that heparin immobilization greatly improves the biocompatibility of the coating material when the LA content is 90% in the copolymers. Hep-Co90 is much more suitable as a drug vehicle for DESs than Co90 and the other two heparinized copolymers, and thus was selected to fabricate As_2O_3-eluting stents. As shown in Fig. 8D, the cross-sectional area stenosis in the arteries treated with Hep-Co90-coated stents was significantly lower (33 ± 5%) than those having the stents coated with Co90 (49 ± 2%, $p = 0.005$), Hep-Co80 (49 ± 4%, $p = 0.033$) and Hep-Co70 (62 ± 5%, $p < 0.001$), whereas no significant difference could be observed between BMSs, Hep-Co90-coated stents and As_2O_3-eluting stents at this time point ($p = 0.697$ between BMSs and Hep-Co90-coated stents; $p = 0.075$ between BMSs and As_2O_3-eluting stents). As shown in Fig. 8A, the corresponding lumen area for BMSs, Hep-Co90-coated stents and As_2O_3-eluting stents was 4.3 ± 0.2, 4.4 ± 0.2 and 5.0 ± 0.2 mm^2, respectively.

At 3 months, neointimal areas and thickness were 2.8 ± 0.4 mm^2, 0.35 ± 0.05 mm; 3.9 ± 0.4 mm^2, 0.52 ± 0.05 mm; 3.0 ± 0.3 mm^2, 0.38 ± 0.04 mm; 4.1 ± 0.2 mm^2, 0.55 ± 0.05 mm; 4.6 ± 0.3 mm^2, 0.66 ± 0.03 mm; and 2.85 ± 0.4 mm^2, 0.24 ± 0.04 mm for BMSs, stents coated with Co90, Hep-Co90, Hep-Co80 and Hep-Co70, and As_2O_3-eluting stents, respectively. The cross-sectional area stenosis of Hep-Co90-coated stents was also significantly lower (45 ± 2%) than the stents coated with Co90 (57 ± 3%, $p = 0.022$), Hep-Co80 (62 ± 3%, $p = 0.018$) and Hep-Co70 (70 ± 2%, $p = 0.001$). There were still no significant differences between BMSs, Hep-Co90-coated stents and As_2O_3-eluting stents at this time point ($p = 0.697$ between BMSs and Hep-Co90-coated stents; $p = 0.188$ between BMSs and As_2O_3-eluting stents). The corresponding lumen area for BMSs, Hep-Co90-coated stents and As_2O_3-eluting stents was 3.8 ± 0.4, 3.7 ± 0.2 and 4.5 ± 0.2 mm^2, respectively.

At 6 months, neointimal areas and thickness were 3.1 ± 0.3 mm^2, 0.40 ± 0.04 mm; 4.2 ± 0.3 mm^2, 0.58 ± 0.04 mm; 3.3 ± 0.3 mm^2, 0.37 ± 0.04 mm; 4.4 ± 0.3 mm^2, 0.61 ± 0.03 mm; 5.4 ± 0.3 mm^2, 0.82 ± 0.03 mm; and 2.3 ± 0.3 mm^2, 0.27 ± 0.04 mm for BMSs, stents coated with Co90, Hep-Co90, Hep-Co80 and Hep-Co70, and As_2O_3-eluting stents, respectively. Generally speaking, neointimal growth after BMS implantation in porcine coronary arteries peaks at 1 month and then decreases for the next 3–6 months [45]. The one-month time point is normally chosen for the maximal intimal

Please cite this article in press as: Gong F et al. Heparin-immobilized polymers as non-inflammatory and non-thrombogenic coating materials for arsenic trioxide eluting stents. Acta Biomater (2009), doi:10.1016/j.actbio.2009.07.013

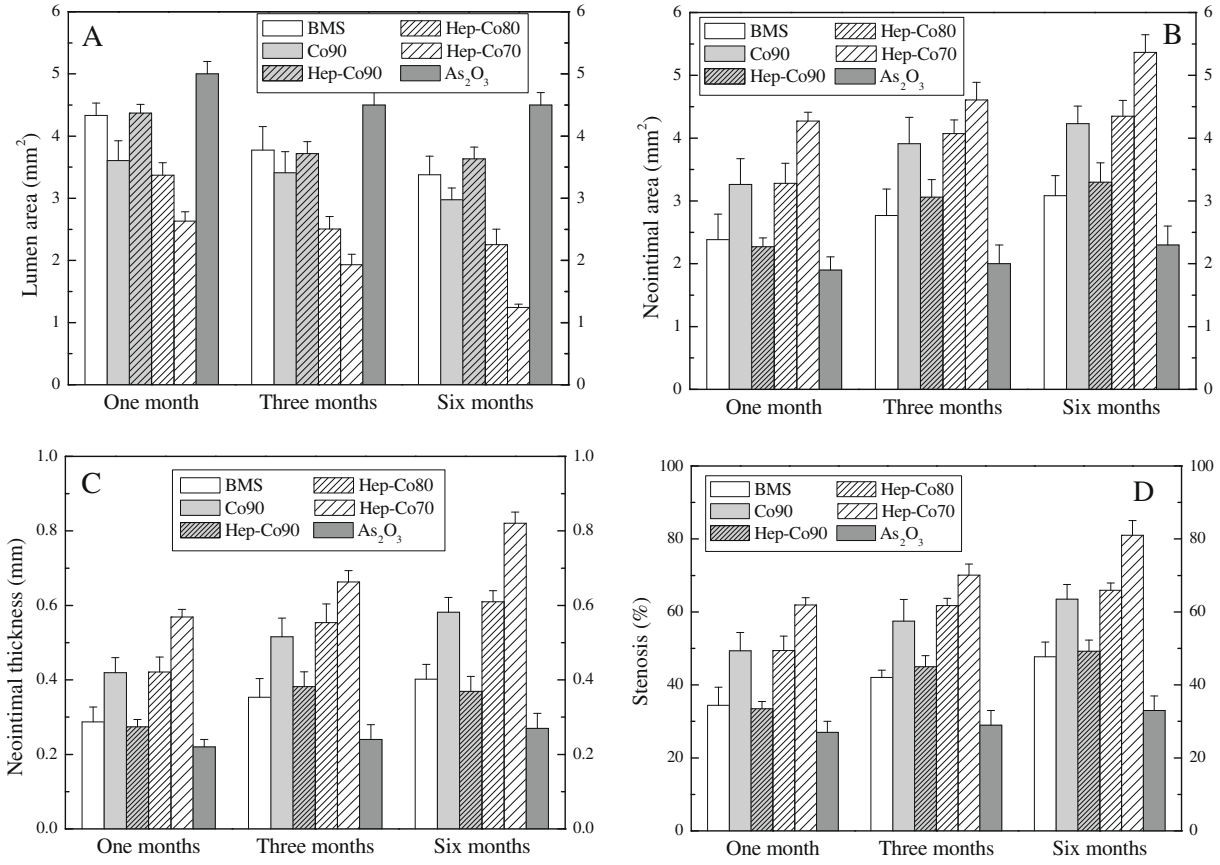

Fig. 8. Histomorphometric analysis on (A) lumen area, (B) neointimal area, (C) neointimal thickness and (D) stenosis of the arteries treated with BMSs, polymer-coated stents and As_2O_3-eluting stents. Results are presented as means ± standard error of the mean ($n = 7$ per group). There are significant differences between Hep-Co90-coated stents and stents coated with Co90, Hep-Co80 and Hep-Co70 at 1, 3 and 6 months ($p < 0.01$). There is no significant difference between BMSs and Hep-Co90-coated stents ($p > 0.05$). There is a significant difference between As_2O_3-eluting stents and BMSs at 6 months ($p < 0.01$).

thickening of BMSs while assessment at later time points can confirm the stability and possible regression of intimal thickening at 3–6 months [45]. In this study, no significant difference ($p > 0.05$) could be observed for BMSs in neointimal area, thickness and stenosis at 1, 3 and 6 months post-implantation. The cross-section area stenosis of Hep-Co90-coated stents (49 ± 2%) was still significantly lower than those of stents coated with Co90 (64 ± 3%, $p = 0.005$), Hep-Co80 (65 ± 4%, $p = 0.006$) and Hep-Co70 (81 ± 4%, $p < 0.001$). The lumen area in the porcine coronary arteries treated with As_2O_3-eluting stents was 32.4% higher than those treated with BMSs, while the neointimal area, neointimal thickness and stenosis all significantly decreased, by factors of 25.8%, 32.5% and 31.2%, respectively.

It is intriguing how As_2O_3-eluting stents could suppress neointimal formation and reduce arterial stenosis up to 6 months considering that the vessel remodeling process lasts for 2–3 months while the drug is completely released within 7 days. It can be tentatively interpreted that the mechanism of elution in As_2O_3-eluting stents is different from those in sirolimus- and paclitaxel-eluting stents. Sirolimus inhibits VSMC proliferation by blocking the cell cycle in the G1 (growth) phase, when RNA is produced and proteins are synthesized [20]. Paclitaxel works by binding to polymerized tubulin, thereby stabilizing it against disassembly and inhibiting cell mitosis (the G2/M phase of cell cycle) [20]. The effects of As_2O_3-eluting stents are associated with a stronger inhibition of VSMC growth and cell cycle, as well as with the induction of apoptosis in VSMCs [20]. VSMC proliferation is a major reason for neointimal hyperplasia after stent implantation [46,47]. As reported earlier [48], the peak of neointimal cell proliferation occurred 1 week after balloon denudation of the rat aorta. It is therefore, critical to inhibit the proliferation of neointimal cells at 1 week after stent implantation. As demonstrated in Fig. 10D, many TUNEL-positive cells were scattered throughout the stented blood vessels with As_2O_3-eluting stents at 7 days post-implantation. The quantification of the TUNEL staining in the stented arteries is shown in Fig. 10E, indicating that TUNEL-positive cells were 65.4 ± 9.1% of the total number of VSMCs in the arteries treated with As_2O_3-eluting stents. In contrast, only 15.1 ± 5.4%, 16.2 ± 6.1% and 18.4 ± 8.7% of VSMCs were TUNEL-positive in the arteries with BMSs, Hep-Co90 and Hep-Co70-coated stents, respectively. Most VSMC apoptosis was observed in the first week after implantation. Consistent with our results, As_2O_3-eluting stents in the previous rabbit model induced more VSMC apoptosis than paclitaxel eluting stents, and VSMC apoptosis was mostly observed in the first week after stent implantation [20]. Drugs that interfere early in the cell cycle (early G1 or pre-G1) are considered to be cytostatic and elicit less cellular necrosis and inflammation than the agents that affect the cell cycle at a later stage [49]. Consistent with the earlier findings [20], As_2O_3 can first inhibit VSMC proliferation by reducing the cells in G1 stage and then induce VSMC apoptosis, which may provide an alternative with potentially lower toxicity.

3.7. Further discussion

Polymer-coated stents developed in this study not only improve the biocompatibility of the stent surface but also control the release of the vasoactive drug, As_2O_3, from the coatings. Neointimal

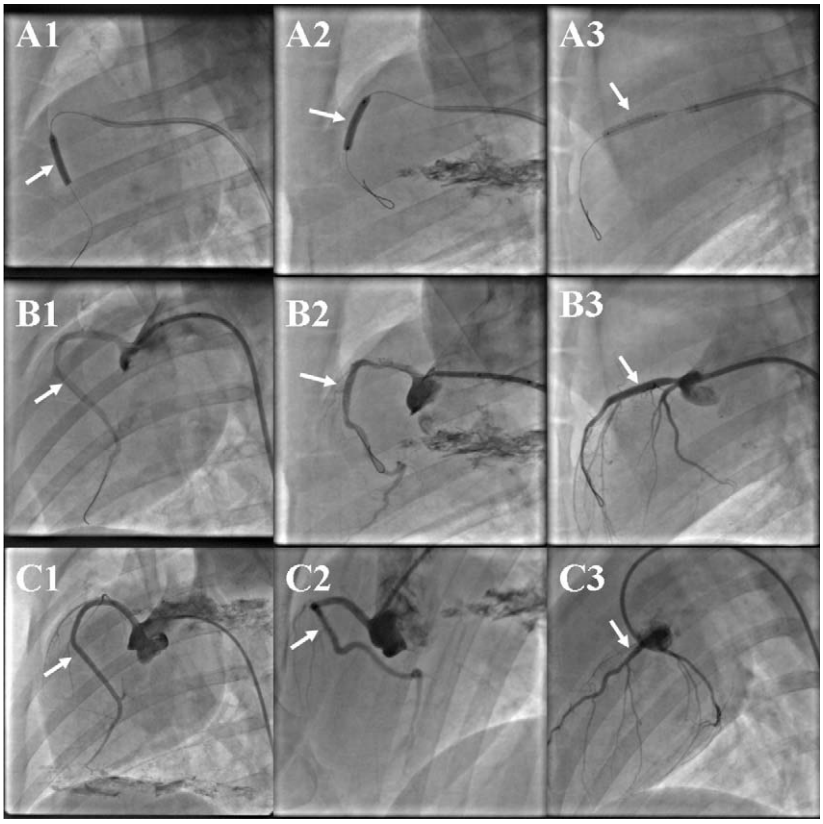

Fig. 9. Angiograms of the coronary arteries after the implantation of As_2O_3-eluting stents. (A) Injury/stent sites with expanded stents; (B) after the procedure; (C) at 1 (C1), 3 (C2) and 6 months (C3) post-implantation. The amount of As_2O_3 was 40 μg per stent. The arrows indicate injury/stent sites.

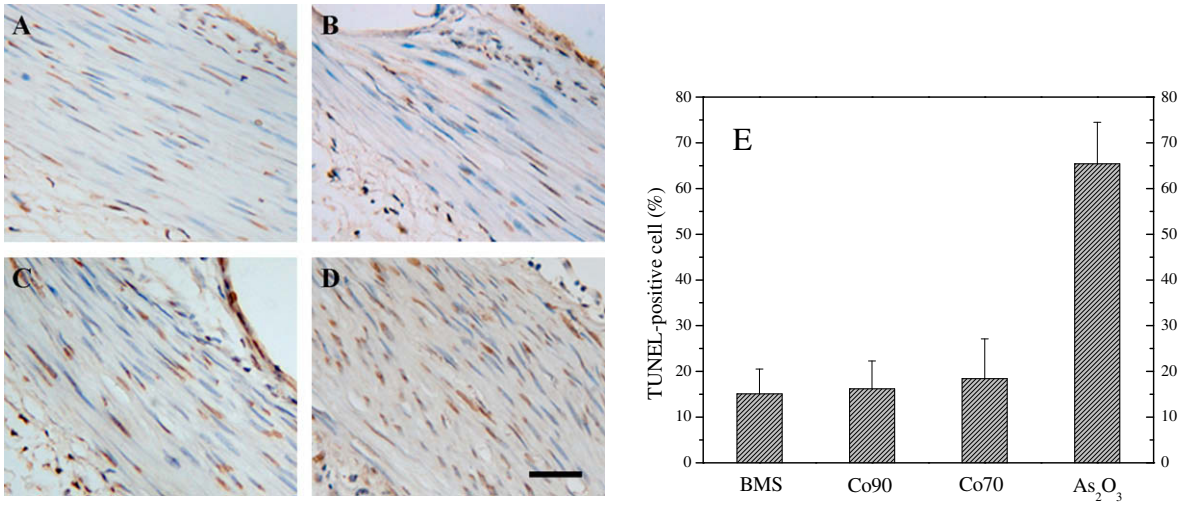

Fig. 10. TUNEL staining of the stented coronary arteries 7 days post-implantation of (A) BMS, (B) Hep-Co90-coated stent, (C) Hep-Co70-coated stent and (D) As_2O_3-eluting stent. Apoptotic cells are indicated by their brown nuclear staining. The sections were counterstained with hematoxylin. The scale bar in D indicates 50 μm and is also applicable for (A–C). (E) Percentage of total cell counts that are TUNEL-positive. There is a significant difference between the As_2O_3-eluting stents and the other stents ($p < 0.01$).

hyperplasia and restenosis are closely related to platelet adhesion, aggregation and thrombus formation [50], while BMSs cause increased intimal thickness, persistent intimal fibrin deposition, intra-intimal hemorrhage, and increased intimal and adventitial inflammation [51,52]. Although no in-stent thrombosis was observed in any stenting groups studied here and the efficacy of the heprinized copolymers in reducing the rate of thrombosis is yet to be tested in vivo, it is evident that heparin immobilization can greatly improve the biocompatibility of the coating material used in DESs. Only a mild lymphohistiocytic reaction of the artery was present in BMSs because BMSs elicited a rather limited inflammatory response of fibromuscular proliferation. Morphologically, there are two types of neointimal proliferation: fibromuscular proliferation and lymphohistiocytic inflammation [43]. The former consists of proliferating mesenchymal spindle cells in a dense collagenous matrix; the latter consists of an active inflammation with lymphocytes and histiocytes, multi-nucleated giant cells and often eosinophils in an edematous matrix of granulation tissue [43]. In

Please cite this article in press as: Gong F et al. Heparin-immobilized polymers as non-inflammatory and non-thrombogenic coating materials for arsenic trioxide eluting stents. Acta Biomater (2009), doi:10.1016/j.actbio.2009.07.013

the stents coated with fast-degrading Hep-Co80 and Hep-Co70, intimal proliferation was severe and belonged to the lymphohistiocytic type. The accumulation of inflammatory cells will stimulate growth factor and cytokine release, which in turn promote neointimal formation and eventually narrow the intra-stent lumen. In Hep-Co90-coated stents with slower degradation, only a mild inflammatory response of the fibromuscular type could be observed up to 6 months. The degree of neointimal proliferation induced by Hep-Co90-coated stents was comparable to that by BMSs, indicating the high potentials of Hep-Co90 as an appropriate biocompatible and biodegradable stent coating material and a carrier for As_2O_3 elution.

For DESs, the amount of coating material plays a pivotal role in foreign body reaction and inflammation formation. Because only 40 μg of As_2O_3 is needed in one As_2O_3-eluting stent, the amount of polymer coating is as tiny as 40–60 μg, which is much lower than those used in sirolimus- and paclitaxel-eluting stents [5,7]. As a result, the inflammatory reaction caused by polymer degradation is expected to be reduced in As_2O_3-eluting stents and consequently the long-term safety and efficacy of such stents could be improved.

4. Conclusions

In summary, three heparin-immobilized biodegradable PLM copolymers of L-lactide (LA) and 5-methyl-5-benzyloxycarbonate-1,3-dioxan-2-one (MBC) with different LA contents (90%, 80% and 70%) have been synthesized and used as biodegradable coating materials to fabricate As_2O_3-eluting stents for inhibiting thrombosis, inflammation and late-stage restenosis. Strong evidence has been presented in porcine coronary arterial implantations that inflammation formation, neointimal hyperplasia and restenosis for biodegradable stent coatings are closely related to their biocompatibility and degradation properties. Heparin immobilization has greatly improved the biocompatibility of the coating polymers. Stents coated with Hep-Co90, a heparinized copolymer with a LA content of 90%, have demonstrated superior results regarding inflammation and foreign body reactions over the stents coated with the precursor copolymer Co90 and other heparinized copolymers with lower LA contents, Hep-Co80 and Hep-Co70. Consequently, Hep-Co90 was chosen as the carrier for As_2O_3 elution. The As_2O_3-eluting stents did not delay healing in a porcine coronary artery injury model. At 1 and 3 months post-implantation, there was no significant difference between BMSs and As_2O_3-eluting stents regarding of the histological parameters, including lumen area, neointimal area, neointimal thickness, and percent neointimal stenosis. At 6 months, As_2O_3-eluting stents significantly reduced neointimal area and thickness compared with BMSs. TUNEL staining of the stented arteries demonstrated that As_2O_3-eluting stents reduced the neointimal hyperplastic response to injury through inhibiting the cell cycle and inducing VSMC apoptosis. Further investigations are necessary to confirm the long-term effects and the effects in inhibiting late-stage thrombosis beyond 6 months, and to define the full pharmacokinetic profile, including dose–response relationships and efficacy in the presence of other treatment regimens. Together with the earlier study using a rabbit iliac artery injury model, this study and preliminary results from human clinical trials suggest that the As_2O_3-eluting stent may represent a useful device in preventing in-stent restenosis.

Acknowledgements

This work was supported by the 863 Project of 2007AA02Z450 from the Ministry of Science and Technology of China. We thank Jianguo Jia, Wei Yang and Ruiming Yao, of the Shanghai Institute of Cardiovascular Diseases, for their help with the animal implantations. We also thank Shanghai Aosi Biological Technology Service Co., Ltd. for help with the histological analysis. The detailed and helpful comments from the reviewers are gratefully appreciated.

Appendix A. Figures with essential colour discrimination

Certain figures in this article, particularly Figs. 4, 5, 7 and 10 are difficult to interpret in black and white. The full colour images can be found in the on-line version, at doi:10.1016/j.actbio.2009.07.013).

References

[1] Fattori R, Piva T. Drug-eluting stents in vascular intervention. The Lancet 2003;361:247–9.
[2] Venkatraman S, Boey F. Release profiles in drug-eluting stents: issues and uncertainties. J Control Release 2007;120:149–60.
[3] Sousa JE, Costa MA, Sousa AGMR. Two-year angiographic and intravascular ultrasound follow-up after implantation of sirolimus-eluting stents in human coronary arteries. Circulation 2003;107:381–3.
[4] Stone GW, Ellis SG, Cox DA. A polymer-based, paclitaxel-eluting stent in patients with coronary arteries diseases. New Eng J Med 2004;350:221–31.
[5] Suzuki T, Kopia G, Hayashi S-I. Stent-based delivery of sirolimus reduces neointimal formation in a porcine coronary model. Circulation 2001;104:1188–93.
[6] Carter AJ, Aggarwal M, Kopia GA. Long-term effects of polymer-based, slow-release, sirolimus-eluting stents in a porcine coronary model. Cardiovasc Res 2004;63:617–24.
[7] Drachman DE, Edelman ER, Seifert P. Neointimal thickening after stent delivery of paclitaxel: change in composition and arrest of growth over 6 months. J Am Coll Cardiol 2000;36:2325–32.
[8] Farb A, Heller PF, Shroff S. Pathological analysis of local delivery of paclitaxel via a polymer-coated stent. Circulation 2001;104:473–9.
[9] Virmani R, Liistro F, Stankovic G. Mechanism of late in-stent restenosis after implantation of a paclitaxel derivate-eluting polymer stent system in humans. Circulation 2002;106:2649–51.
[10] Pfisterer M, Brunner L, Rocca HP, Buser PT. Late clinical events after clopidrogel discontinuation may limit the benefit of drug-eluting stents. J Am Coll Cardiol 2006;48:2584–91.
[11] Stone GW, Moses JW, Ellis SG. Safety and efficacy of sirolimus and paclitaxel-eluting coronary stents. New Eng J Med 2007;356:998–1008.
[12] Mauri L, Hsieh WH, Massaro JM. Stent thrombosis in randomized clinical trials of drug-eluting stents. New Eng J Med 2007;356:1020–9.
[13] Eisenstein EL, Anstrom KJ, Kong DF. Clopidrogel use and long term clinical outcomes after drug-eluting stent implantation. J Am Med Assoc 2007;297:159–68.
[14] Kotani J, Awata M, Nanto S. Incomplete neo-intimal coverage of sirolimus-eluting stents: angioscopic findings. J Am Coll Cardiol 2006;47:2108–11.
[15] Ong ATL, Serruys PW. Technology insight: an overview of research in drug-eluting stents. Nat Clin Prac Cardiovasc Med 2005;2:647–58.
[16] Welt FG, Rogers C. Inflammation and restenosis in the stent era. Arterioscler Thromb Vasc 2002;22:1769–76.
[17] Capila I, Linhardt RJ. Heparin protein interactions. Angew Chem Inter Ed 2002;41:390–412.
[18] DeScheerder I, Wang K, Wilczek K, Meuleman D, VanAmsterdam R, Vogel G, et al. Experimental study of thrombogenicity and foreign body reaction induced by heparin-coated coronary stents. Circulation 1997;95:1549–53.
[19] Blezer R, Cahalan L, Cahalan PT. Heparin coating of tantalum coronary stents reduces surface thrombin generation but not factor IXa generation. Blood Coagul Fibrin 1998;9:435–40.
[20] Yang W, Ge J, Liu H, Zhao K, Liu X, Qu X, et al. Arsenic trioxide eluting stent reduces neointimal formation in a rabbit iliac artery injury model. Cardiovas Res 2006;72:483–93.
[21] Al-Azemi TalalF, Kirpal SB. Novel functional polycarbonate by lipase-catalyzed ring-opening polymerization of 5-methyl-5-benzyloxycarbonyl-1,3-dioxan-2-one. Macromolecules 1999;32:6536–40.
[22] Jee KS, Park HD, Park KD, Kim YH, Shin JW. Heparin conjugated polylactide as a blood compatible material. Biomacromolecules 2004;5:1877–81.
[23] Xu FJ, Li YL, Kang ET, Neoh KG. Heparin-coupled poly(poly(ethylene glycol) monomethacrylate)-Si(111) hybrids and their blood compatible surfaces. Biomacromolecules 2005;6:1759–68.
[24] Wang S, Kempen DH, Simha NK, Lewis JL, Windebank AJ, Yaszemski MJ, et al. Photo-cross-linked hybrid polymer networks consisting of poly(propylene fumarate) and poly(caprolacton fumarate): controlled physical properties and regulated bone and nerve cell responses. Biomacromolecules 2008;9:1229–41.
[25] Wang S, Yaszemski MJ, Knight AM, Gruetzmacher JA, Windebank AJ, Lu L. Photo-crosslinked poly(ε-caprolactone fumarate) networks for guided peripheral nerve regeneration: material properties and preliminary biological evaluations. Acta Biomater 2009;5:1531–42.

[26] Ranade SV, Miller KM, Richard RE. Physical characterization of controlled release of paclitaxel from the TAXUS™ Express²™ drug-eluting stent. J Biomed Mater Res 2004;71(A):625–34.
[27] Dibra A, Kastrati A, Mehilli J. Influence of stent surface topography on the outcomes of patients undergoing coronary stenting: a randomized double-blind controlled trial. Cath Cardiovasc Interven 2005;65:374–80.
[28] Hara H, Nakamura M, Palmaz JC, Schwartz RS. Role of stent design and coatings on restenosis and thrombosis. Adv Drug Delivery Rev 2006;58:377–86.
[29] Park K, Mao FW, Park H. Morphological characterization of surface-induced platelet activation. Biomaterials 1990;11:24–31.
[30] Wang D-A, Ji J, Gao C-Y, Yu G-H, Feng L-X. Surface coating of stearyl poly(ethylene oxide) coupling-polymer on polyurethane guiding catheters with poly(ether urethane) film-building additive for biomedical applications. Biomaterials 2001;22:1549–62.
[31] Hardhammar PA, van Beusekom HMM, Emanuelsson HU, Hofma SH, Albertsson PA, Verdouw PD, et al. Reduction in thrombotic events with heparin-coated Palmaz–Schatz stents in normal porcine coronary arteries. Circulation 1996;93:423–30.
[32] Tamai H, Igaki K, Kyo E. Initial and 6-month results of biodegradable poly-L-lactic acid coronary stents in humans. Circulation 2000;102:399–404.
[33] Joner M, Nakazawa G, Finn AV, Quee SC, Coleman L, Acampado E, et al. Endothelial cell recovery between comparator polymer-based drug-eluting stents. J Am Coll Cardiol 2008;52:333–42.
[34] Finn AV, Kolodgie FD, Harnek J, Guerrero LJ, Acampado E, Tefera K, et al. Differential response of delayed healing and persistent inflammation at sites of overlapping sirolimus- or paclitaxel-eluting stents. Circulation 2005;112:270–8.
[35] Hofma SH, van der Giessen WJ, van Dalen BM. Indication of long-term endothelial dysfunction after sirolimus-eluting stent implantation. Eur Heart J 2006;27:166–70.
[36] Togni M, Windecker S, Cocchia R. Sirolimus-eluting stents associated with paradoxic coronary vasoconstriction. J Am Coll Cardiol 2005;46:231–6.
[37] Sousa JE, Costa MA, Farb A. Vascular healing 4 years after the implantation of sirolimus-eluting stent in humans. Circulation 2001;110:e5–6.
[38] Kang IK, Kwon OH, Kim MK, Lee YM, Sung YK. In vitro blood compatibility of functional group grafted and heparin-immobilized polyurethanes prepared by plasma glow discharge. Biomaterials 1997;18:1099–107.
[39] Koromila G, Michanetzis GPA, Missirlis YF, Antimisiaris SG. Heparin incorporating liposomes as a delivery system of heparin from PET-covered metallic stents: effect on hemocompatibility. Biomaterials 2006;27:2525–33.
[40] Beythien C, Gutensohn K, Bau J, Hamm CW, Kuhnl P, Meinertz T, et al. Influence of stent length and heparin coating on platelet activation: a flow cytometric analysis in a pulsed floating model. Thromb Res 1999;94:79–86.
[41] Christensen K, Larsson R, Emanuelsson H, Elgue G, Larsson A. Improved blood compatibility of a stent graft by combining heparin coating and abciximab. Thromb Res 2005;11:245–53.
[42] Riedl CR, Witkowski M, Plas E, Pflueger H. Heparin coating reduces encrustation of ureteral stents: a preliminary report. Int J Antimicrob Ag 2002;19:507–10.
[43] De Scheerder IK, Wilczek KL, Verbeken EV. Biocompatibility of polymer-coated oversized metallic stents implanted in normal porcine coronary arteries. Atherosclerosis 1995;114:105–14.
[44] Lincoff MA, Furst JG, Ellis SG, Tuch RJ, Topol EJ. Sustained local delivery of Dexamethasone by a novel intravascular eluting stent to prevent restenosis in the porcine coronary injury model. J Am Coll Cardiol 1997;29:808–16.
[45] Nakazawa G, Finn AV, John MC, Kolodgie FD, Virmani R. The significance of preclinical evaluation of sirolimus-, paclitaxel-, and zotarolimus-eluting stents. Am J Cardiol 2007;100(8B):36M–44M.
[46] Schwartz RS, Holmes Jr DR, Topol EJ. The restenosis paradigm revisited: an alternative proposal for cellular mechanisms. J Am Coll Cardiol 1992;20:1284–93.
[47] Karas SP, Gravanis MB, Santorian EC, Robinson KA, Anderberg KA, King SB. Coronary intimal proliferation after balloon injury and stenting in swine: an animal model of restenosis. J Am Coll Cardiol 1992;20:467–74.
[48] Zeymer U, Fishbein MC, Forrester JS, Cercek B. Proliferating cell nuclear antigen immunohistochemistry in rat aorta after balloon denudation: comparison with thymidine and bromodeoxyuridine labeling. Am J Pathol 1992;141:685–90.
[49] Braun-Dullaeus RC, Mann MJ, Dzau VJ. Cell cycle progression: new therapeutic target for vascular proliferative disease. Circulation 1998;98:82–9.
[50] Ellis JT, Kilpatrick DL, Consigny P, Prabhu S, Hossainy SFA. Therapy considerations in drug-eluting stents. Crit Rev Ther Drug Carr Sys. 2004;22:1–25.
[51] Castagna MT, Mintz GS, Leiboff BO, Ahmed JM, Mehran R, Satler LF, et al. The contribution of mechanical problems to in-stent restenosis: an intravascular ultrasonographic analysis of 1090-consecutive in-stent restenosis lesions. Am Heart J 2001;142:970–4.
[52] Sabate M, Costa MA, Kozuma K, Kay IP, van der Giessen WJ, Coen VL, et al. Geographic miss: a cause of treatment failure in radiooncology applied to intracoronary radiation therapy. Circulation 2000;101:2467–71.

Please cite this article in press as: Gong F et al. Heparin-immobilized polymers as non-inflammatory and non-thrombogenic coating materials for arsenic trioxide eluting stents. Acta Biomater (2009), doi:10.1016/j.actbio.2009.07.013